Editors' Suggestion

Non-Hermitian Fermi-Dirac Distribution in Persistent Current Transport

Pei-Xin Shen,[1,2,*] Zhide Lu,[2] Jose L. Lado,[3] and Mircea Trif[1,†]

[1]*International Research Centre MagTop, Institute of Physics, Polish Academy of Sciences, Aleja Lotnikow 32/46, PL-02668 Warsaw, Poland*

[2]*Institute for Interdisciplinary Information Sciences, Tsinghua University, Beijing 100084, China*

[3]*Department of Applied Physics, Aalto University, FI-00076 Aalto, Espoo, Finland*

(Received 28 March 2024; revised 6 June 2024; accepted 19 July 2024; published 23 August 2024)

Persistent currents circulate continuously without requiring external power sources. Here, we extend their theory to include dissipation within the framework of non-Hermitian quantum Hamiltonians. Using Green's function formalism, we introduce a non-Hermitian Fermi-Dirac distribution and derive an analytical expression for the persistent current that relies solely on the complex spectrum. We apply our formula to two dissipative models supporting persistent currents: (i) a phase-biased superconducting-normal-superconducting junction; (ii) a normal ring threaded by a magnetic flux. We show that the persistent currents in both systems exhibit no anomalies at any emergent exceptional points, whose signatures are only discernible in the current susceptibility. We validate our findings by exact diagonalization and extend them to account for finite temperatures and interaction effects. Our formalism offers a general framework for computing quantum many-body observables of non-Hermitian systems in equilibrium, with potential extensions to nonequilibrium scenarios.

DOI: 10.1103/PhysRevLett.133.086301

Introduction—Recent intensive research in non-Hermitian (NH) physics [1–4] has revealed intriguing phenomena in both the classical [5–9] and quantum realms [10–12]. The biorthogonal and non-Bloch frameworks have reshaped the conventional bulk-edge correspondence [13–16], while the symmetry classifications of the NH matrices have enriched the topological phases compared to their Hermitian counterparts [17–21]. Exceptional points (EPs), where the NH Hamiltonian is not diagonalizable [22–24], can enhance sensing capabilities [25–28] and trigger new critical phenomena [29–32].

In the field of open quantum systems, NH physics is instrumental in characterizing the dissipative nature of systems [33–35]. The Lindblad formalism [36–39] provides routes to address system-reservoir interactions. By neglecting quantum jumps or focusing on Gaussian systems [40–42], the dynamics is dictated solely by an effective NH Hamiltonian $\mathcal{H}_{\mathrm{eff}}$. The Green's function formalism presents an alternative path to $\mathcal{H}_{\mathrm{eff}}$ by integrating out external reservoirs $\mathbb{E}$ to include complex self-energies $\Sigma \neq \Sigma^{\dagger}$ [43–48]. Although the spectral properties of $\mathcal{H}_{\mathrm{eff}}$ have been extensively explored, quantum many-body observables [49], such as the supercurrents in phase-biased superconducting–normal–superconducting (SNS) junctions shown in Fig. 1(a), are currently under active discussion. Existing approaches, such as the derivative of complex eigenvalues [50,51] and the expectation values obtained from the left-right (LR) or right-right (RR) eigenvectors [52], often yield anomalies at EPs [53], calling for a microscopic approach to grasp the subtleties of the NH persistent current transport.

In this Letter, we provide a resolution to this conundrum grounded on a NH Fermi-Dirac distribution associated with the biorthogonal single-particle eigenstates. We find that the supercurrent $I(\phi)$ in an SNS junction biased by a phase ϕ and coupled to reservoirs is given by (in units of $e/\hbar$):

$$I(\phi) = -\frac{1}{\pi}\frac{\mathrm{d}}{\mathrm{d}\phi}\mathrm{Im}\mathrm{Tr}(\mathcal{H}_{\mathrm{eff}}\ln\mathcal{H}_{\mathrm{eff}}). \tag{1}$$

This formula is derived in the wide-band limit, which is nonperturbative and can also accurately describe the strong coupling regime. Moreover, it also applies to the persistent current in a normal mesoscopic ring threaded by a magnetic flux, as shown in Fig. 1(b). Our results align with the exact diagonalization of the full Hermitian system including the reservoir and do not exhibit any singularities at EPs for both models [see Figs. 1(c) and 1(d)]. We further generalize Eq. (1) to finite temperatures and find that persistent currents are reduced, which is also observed when many-body interactions are taken into account. Finally, as shown in Fig. 4, the signatures of EPs can instead become evident in the current susceptibility associated with response to an *ac* phase bias drive. Our formalism not only clarifies the behavior of persistent currents in fermionic NH systems but also

[*]Contact author: peixin.shen@outlook.com

[†]Contact author: mtrif@magtop.ifpan.edu.pl

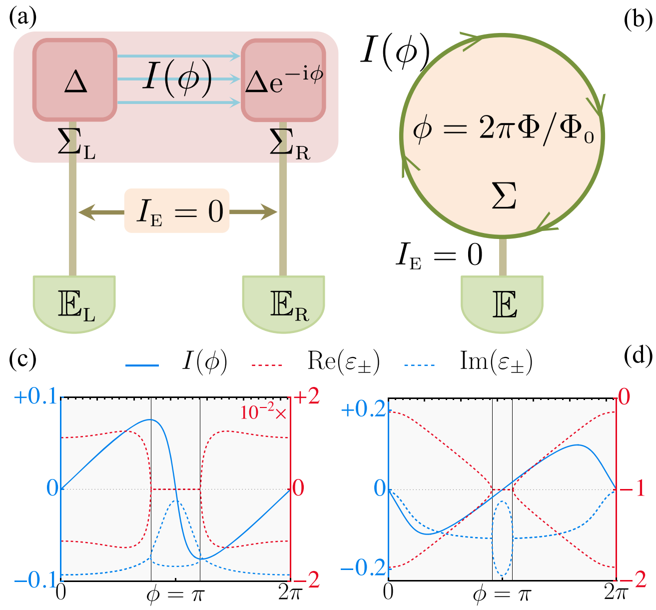

FIG. 1. Schematic of systems coupled to external reservoirs $\mathbb{E}$: (a) an SNS junction with a phase bias ϕ; (b) a normal metallic ring threaded by normalized magnetic flux ϕ. Each system is characterized by an effective NH Hamiltonian $\mathcal{H}_{\rm eff}$ that includes a complex self-energy Σ from $\mathbb{E}$. In equilibrium, both models maintain persistent currents $I(\phi)$ and zero leakage currents $I_{\rm E}$. (c) and (d) Complex spectra $\varepsilon_\pm$ showing EPs around π (black lines) and persistent current $I(\phi)$ as a function of ϕ. The current $I(\phi)$ calculated using Eq. (1) shows no signs of singularity at the EPs. Parameters: (c) $N_{\rm L} = N_{\rm M} = N_{\rm R} = 4$, $N_{\rm E} = 101$, $t = -\Delta = -1$, $\kappa = 0.4t$, $\mu = g = -1.1$; (d) $N = 6$, $N_{\rm E} = 101$, $t = \kappa = \mu = -1$, $g = 0$, $t_i \sim t * \mathrm{Unif}(0.7, 1.3)$.

sets the stage for analyzing other quantum many-body observables with dissipation.

Phenomenology and methodology—Initially, we outline a heuristic explanation of our main findings, deferring the technical details to subsequent sections and the Supplemental Material [54]. We focus, for simplicity, on spinless fermionic systems with Hamiltonians that depend on a parameter ϕ, such as in phase-biased SNS junctions $H_{\rm sys}(\phi) = \vec{C}^\dagger \mathcal{H}_{\rm sys}(\phi)\vec{C}/\mathbf{2}$, where $\mathcal{H}_{\rm sys}(\phi)$ is the Bogoliubov–de Gennes (BdG) Hamiltonian, $\vec{C} = (c_1, \ldots, c_{\rm N}, c_1^\dagger, \ldots, c_{\rm N}^\dagger)^{\rm T}$ is a $\mathbf{2}N$-dimensional spinor, and $c_j^\dagger$ (c_j) is the fermionic creation (annihilation) operator at site j. The discussion below also applies to normal metals described by $\mathcal{H}_{\rm sys}(\phi)$ on an N-dimensional basis $\vec{C} = (c_1, \ldots, c_{\rm N})^{\rm T}$, substituting $\mathbf{2}$ for $\mathbf{1}$. For brevity, we will use calligraphy to denote the first quantized operators and omit the explicit dependence on ϕ in our notation for Hamiltonians, eigenvalues, and eigenvectors hereafter.

For isolated and Hermitian systems $\mathcal{H}_{\rm sys}$, the persistent current $I_{\rm iso}(\phi)$ n the many-body ground state with energy E_0 follows [56],

$$I_{\rm iso}(\phi) = \mathbf{2}\frac{dE_0}{d\phi} = \sum_{\epsilon_n \leqslant 0} \frac{d\epsilon_n}{d\phi} = \sum_{\epsilon_n \leqslant 0} \frac{\langle \psi_n | \mathcal{J} | \psi_n \rangle}{\mathbf{2}}, \quad (2)$$

where the factor of 2 stems from the Cooper pair, $J = \vec{C}^\dagger \mathcal{J} \vec{C}/\mathbf{2}$ is the persistent current operator, ϵ_n and $|\psi_n\rangle$ are eigenvalues and eigenstates of $\mathcal{H}_{\rm sys}$. Given the local conservation law of $n_j = c_j^\dagger c_j$ in the $\mathbb{N}$ segment (e.g., the normal part in SNS junctions), the site-resolved current operator [35], $J_j = -it_j(c_j^\dagger c_{j+1} - c_{j+1}^\dagger c_j)$, follows the continuity equation in equilibrium: $0 = \langle \dot{n}_j \rangle = i\langle [H_{\rm sys}, n_j] \rangle = \langle J_j \rangle - \langle J_{j-1} \rangle$, $\forall\, j \in \mathbb{N}$, where t_j is the hopping strength at site j. Therefore, we set $J \equiv J_j$ at the first site of $\mathbb{N}$ and omit the subscript.

To account for dissipation, we couple the system to a thermal reservoir $\mathbb{E}$. In the long-time limit, the system reaches equilibrium and $\mathbb{E}$ acts as a source of dephasing [57–65]. This coupling leads to the emergence of a complex self-energy $\Sigma(\omega)$ in the system. In the wide-band limit $\Sigma(\omega) \approx \Sigma(0)$ [66–68], the system is effectively described by the NH Hamiltonian $\mathcal{H}_{\rm eff} \equiv \mathcal{H}_{\rm sys} + \Sigma(0)$, which exhibits a complex spectrum ε_n with $\mathrm{Im}\varepsilon_n \leqslant 0$ and supports biorthogonal single-particle modes [69]: $\mathcal{H}_{\rm eff}|\psi_n^{\rm R}\rangle = \varepsilon_n |\psi_n^{\rm R}\rangle$, $\mathcal{H}_{\rm eff}^\dagger |\psi_n^{\rm L}\rangle = \varepsilon_n^* |\psi_n^{\rm L}\rangle$, and $\langle \psi_n^{\rm L} | \psi_m^{\rm R} \rangle = \delta_{nm}$. Using this biorthogonal basis, we represent the retarded Green's function of the system as [70–72]

$$G_{\rm sys}(\omega) = \frac{1}{\omega - \mathcal{H}_{\rm eff}} = \sum_n \frac{|\psi_n^{\rm R}\rangle\langle \psi_n^{\rm L}|}{\omega - \varepsilon_n}, \quad (3)$$

and obtain the density of states operator $\rho(\omega) = i[G_{\rm sys}(\omega) - G_{\rm sys}^\dagger(\omega)]/2\pi$. In thermal equilibrium, any correlator can be calculated by $\langle c_i^\dagger c_j \rangle = \int \langle j|\rho(\omega)|i\rangle \times f_{\rm FD}(\omega)d\omega$, where $f_{\rm FD}(\omega)$ is the Fermi-Dirac distribution of the entire system. Given $f_{\rm FD}(\omega) = \Theta(-\omega)$ at zero temperature, we derive an analytical correlator $\langle c_i^\dagger c_j \rangle$ by integrating over ω:

$$\langle c_i^\dagger c_j \rangle = \frac{i}{2\pi} \sum_n \left(\psi_{ni}^{\rm L*} \psi_{nj}^{\rm R} \ln \varepsilon_n - \psi_{ni}^{\rm R*} \psi_{nj}^{\rm L} \ln \varepsilon_n^* \right), \quad (4)$$

where $\psi_{nj}^{\rm L/R} \equiv \langle j | \psi_n^{\rm L/R} \rangle$, $\ln \varepsilon_n \equiv \ln|\varepsilon_n| + i \arg \varepsilon_n$ and $-\pi \leqslant \arg \varepsilon_n \leqslant 0$ [73]. Similarly, $\langle c_i c_j \rangle$ is obtained by replacing i with $N + i$ on the right-hand side of Eq. (4). Therefore, the expectation value of a general quadratic Hermitian operator $O = \vec{C}^\dagger \mathcal{O} \vec{C}/\mathbf{2}$ is [54]

$$\langle O \rangle = \mathrm{Im} \sum_n \frac{\langle \mathcal{O} \rangle_n^{\rm LR} f_{\rm eff}(\varepsilon_n)}{\mathbf{2}} = \frac{\mathrm{Im}\mathrm{Tr}[\mathcal{O} f_{\rm eff}(\mathcal{H}_{\rm eff})]}{\mathbf{2}}, \quad (5)$$

where $\langle \mathcal{O} \rangle_n^{\rm LR} \equiv \langle \psi_n^{\rm L} | \mathcal{O} | \psi_n^{\rm R} \rangle$ and $f_{\rm eff}(\varepsilon) \equiv -(1/\pi)\ln\varepsilon$ acts as a Fermi-Dirac distribution for NH systems, whose imaginary part reduces to $\Theta(-\varepsilon)$ as $\mathrm{Im}\varepsilon \to 0$ [74].

Equation (5) represents one of our main results and remains continuous at EPs [75]. The persistent current can be calculated by substituting $\mathcal{O}$ with $\mathcal{J}$ in Eq. (5). Furthermore, applying the identity $\langle\mathcal{J}\rangle_n^{\mathrm{LR}} = \mathbf{2}\partial_\phi\varepsilon_n$ for each biorthogonal single-particle mode and rearranging the derivatives, one can obtain Eq. (1) and verify that it recovers Eq. (2) in the Hermitian limit. It is important to emphasize that our Eq. (1) is distinct from a simple continuation of Eq. (2) to complex eigenvalues $\sum_{\mathrm{Re}\varepsilon_n\leqslant 0}\partial_\phi\varepsilon_n$ (or, equivalently, the LR-basis current $I_{\mathrm{LR}}(\phi)\equiv\sum_{\mathrm{Re}\varepsilon_n\leqslant 0}\langle\mathcal{J}\rangle_n^{\mathrm{LR}}/\mathbf{2}$) recently proposed in Refs. [50–52], as well as the RR-basis current $I_{\mathrm{RR}}(\phi)\equiv\sum_{\mathrm{Re}\varepsilon_n\leqslant 0}\langle\mathcal{J}\rangle_n^{\mathrm{RR}}/\mathbf{2}$ widely adopted with postselection [76–78]. As demonstrated below, both of these definitions fail to accurately describe the persistent current in equilibrium, whereas Eq. (1) is in full agreement with the exact diagonalization.

Model reservoir and self-energy—To validate our findings, we connect the system H_{sys} to an N_{E}-site fermionic reservoir $H_{\mathrm{res}} = \sum_j[(tc_j^\dagger c_{j+1} + \mathrm{H.c.}) + gc_j^\dagger c_j]$, where $t<0$ is the hopping strength and g is the chemical potential. This specific reservoir is chosen for its dual analytical and numerical merits. First, connecting one end of $\mathbb{E}$ to the l site of the system via $H_{\mathrm{tun}} = \kappa(c_{N_{\mathrm{E}}}^\dagger c_l + c_l^\dagger c_{N_{\mathrm{E}}})$ with coupling strength $\kappa<0$ will induce a self-energy $\Sigma_l(0) = \Sigma(0)\otimes|l\rangle\langle l|$ onto $\mathcal{H}_{\mathrm{sys}}$, where $\Sigma(0) = -\kappa^2/t^2[\tau_z g/2 + \mathrm{i}\sqrt{t^2-(g/2)^2}]$ and τ_z is the Pauli-Z matrix acting in the particle-hole space [34]. This expression is exact when $N_{\mathrm{E}}\to\infty$ and also applies to normal metals upon removal of τ_z [54]. Second, the tight-binding form of H_{res} allows us to compare Eqs. (1) and (2) by performing an exact diagonalization of the entire Hermitian system $H_{\mathrm{tot}} = H_{\mathrm{sys}} + H_{\mathrm{res}} + H_{\mathrm{tun}}$. Next, we apply this benchmark framework to two concrete NH models: a phase-biased SNS junction and a normal ring threaded by a magnetic flux.

NH SNS junctions—The SNS junction is a pivotal platform for quantum transport, whose Hamiltonian reads

$$H_{\mathrm{SNS}} = \sum_j\left(t_jc_j^\dagger c_{j+1} + \Delta_j\mathrm{e}^{-\mathrm{i}\phi_j}c_j^\dagger c_{j+1}^\dagger + \mathrm{H.c.}\right) + \mu c_j^\dagger c_j, \quad (6)$$

where Δ_j is the superconducting gap with phase ϕ_j at site j, μ is the chemical potential and $t_j = t$. The number of sites in the left, middle, and right parts is $N_{\mathrm{L}}, N_{\mathrm{M}}, N_{\mathrm{R}}$, respectively. The middle segment is normal metal by setting $\Delta_j = \phi_j = 0,\ \forall\ j\in\mathbb{N}\equiv[N_{\mathrm{L}}, N_{\mathrm{L}}+N_{\mathrm{M}}]$. The outer segments are superconductors $\Delta_j = \Delta\neq 0$ with phase bias applied such that $\phi_j = \phi$ in the right segment and $\phi_j = 0$ in the left segment.

As depicted in Fig. 1(a), the SNS junction incorporates self-energies $\Sigma_{\mathrm{L}} = \Sigma_1(0)$ and $\Sigma_{\mathrm{R}} = \Sigma_{\mathrm{N}}(0)$, after being connected to two separate reservoirs at its ends. This results in an effective NH Hamiltonian $\mathcal{H}_{\mathrm{eff}} = \mathcal{H}_{\mathrm{SNS}} + \Sigma_{\mathrm{L}} + \Sigma_{\mathrm{R}}$, whose spectrum exhibits pairs $(+\varepsilon_n, -\varepsilon_n^*)$ pertaining to the particle-hole symmetry of NH systems [18]. Figure 1(c) highlights a pair of complex spectra $\varepsilon_\pm$ with EPs near $\phi=\pi$, where $\mathrm{Re}\varepsilon_\pm$ are pinned to zero. The calculation of supercurrents in the presence of EPs has recently garnered attention and sparked ongoing debates. As mentioned above, considering $\langle\mathcal{J}\rangle_n^{\mathrm{LR}} = \mathbf{2}\partial_\phi\varepsilon_n$, a simple generalization of Eq. (2) to complex eigenvalues $\sum_{\mathrm{Re}\varepsilon_n\leqslant 0}\partial_\phi\varepsilon_n$ [50,51] is equivalent to the LR-basis current $I_{\mathrm{LR}}(\phi)$ [52]. However, as shown in Fig. 2(a), this approach results in a divergent supercurrent due to the nondifferentiable nature of EPs. On the other hand, the RR-basis current $I_{\mathrm{RR}}(\phi)$ has a finite but nonsmooth value at EPs, and also exhibits asymmetry around π. Furthermore, $I_{\mathrm{RR}}(\phi)$ does not adhere to the local conservation law and will show distinct curves for different $j\in\mathbb{N}$ (see Supplemental Material [54] for details). In stark contrast, the current $I(\phi)$ computed by Eq. (1) exhibits no anomalies at EPs. It matches excellently with the current calculated from Eq. (2) by exact diagonalization for the entire Hermitian H_{tot} with a large reservoir. Compared to current $I_{\mathrm{iso}}(\phi)$ in an isolated SNS junction, we observe an enhancement in $I(\phi)$ within the moderate coupling regime $\kappa = 0.4t$. This seemingly counterintuitive effect arises because the lower-energy mode ε_- has a negative contribution to the current, which is effectively balanced by ε_+ due to level broadening in the NH case. However, as κ/t increases, $I(\phi)$ starts to decrease, since dissipation also suppresses the positive current contribution from other states [54].

NH normal rings—A mesoscopic ring threaded by a magnetic flux Φ also carries a persistent current because the coherence length of the wave function extends over

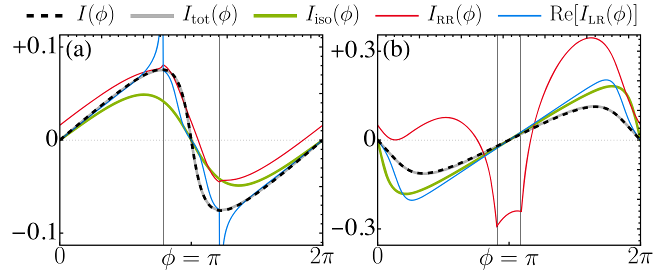

FIG. 2. Methodological comparisons of persistent currents in two NH systems: (a) a phase-biased SNS junction; (b) a normal ring threaded by a magnetic flux. The current $I(\phi)$ (dashed) computed by Eq. (1) matches the exact diagonalization (gray) of the full Hermitian system. The isolated system (green) acts as a reference, showing an enhanced (reduced) current for the SNS (ring) model upon coupling to reservoirs. In (a), LR-basis currents (blue) diverge at the EPs (black lines), a feature not observed in (b), where a pair of EP modes $\varepsilon_\pm$ cancel out the divergence. RR-basis currents (red) violate the local conservation law and exhibit asymmetry around π. The parameters are the same as in Fig. 1.

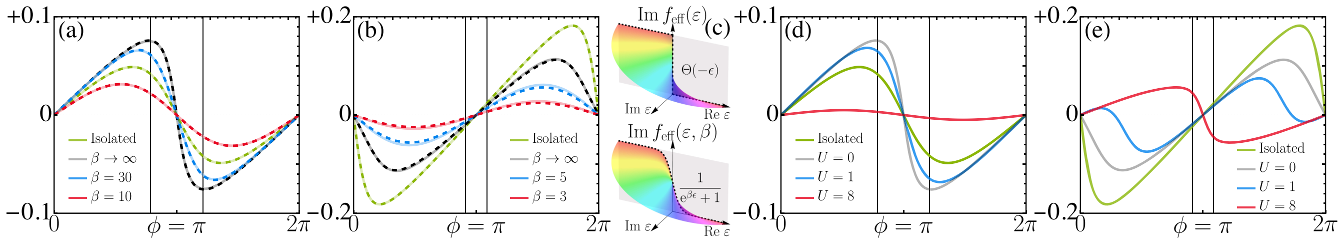

FIG. 3. Effects of temperature and interactions on persistent currents $I(\phi)$ in NH systems. Panels (a) and (b) display $I(\phi)$ at finite temperatures $\beta = 1/k_B T$ for an SNS junction and a mesoscopic ring, compared to isolated systems at $T = 0$ (green). The currents computed using Eq. (9) (dashed) are consistent with the exact diagonalization (solid), indicating a decrease in $I(\phi)$ as T increases. (c) Illustration of the imaginary part of the NH Fermi-Dirac distribution at zero and finite temperatures, where $\mathrm{Im} f_{\mathrm{eff}}(\varepsilon, \beta)$ in Eq. (8) will reduce to the conventional Fermi-Dirac distribution (dashed) as $\mathrm{Im}\varepsilon \to 0$. In (d) and (e), many-body interactions are shown to suppress the amplitude of $I(\phi)$ in both systems. The parameters are as in Fig. 1. No singularities are found at EPs (black lines) in all cases presented.

its entire circumference [79–83]. The gauge-invariant tight-binding Hamiltonian is given by [84–86]

$$H_{\mathrm{ring}} = \sum_j \left(t_j e^{-i\phi_j} c_j^\dagger c_{j+1} + \mathrm{H.c.} \right) + \mu c_j^\dagger c_j, \tag{7}$$

where the normalized magnetic flux $\phi_N = \phi = 2\pi\Phi/\Phi_0$ is placed between the Nth and first site, leaving other $\phi_j = 0$. Here, $\Phi_0 = h/e$ is the flux quantum that reflects the periodicity of Eq. (7) in the flux Φ [87]. We account for elastic scatterings by assigning uniformly random hopping strengths along the ring [88]. However, since the local conservation law spans the whole ring, $\langle J_j \rangle$ remains uniform across all sites.

As illustrated in Fig. 1(b), the fermionic reservoir is connected to a single site within the ring [89], inducing a self-energy $\Sigma \equiv \Sigma_N(0)$. Consequently, the ring is described by $\mathcal{H}_{\mathrm{eff}} = \mathcal{H}_{\mathrm{ring}} + \Sigma$. When $\mu = 0$, similar to the SNS junctions, the LR-basis current $I_{\mathrm{LR}}(\phi)$ of the ring will diverge at EPs near $\phi = \pi$. Here, in order to explore different impacts of EPs, we set $\mu = -1$ and shift two EP modes $\varepsilon_\pm$ below the Fermi level, as depicted in Fig. 1(d). Since $\varepsilon_\pm$ contribute to $I_{\mathrm{LR}}(\phi)$ in pairs, their divergences cancel out, resulting in a smooth curvature for $I_{\mathrm{LR}}(\phi)$ in Fig. 2(b). The RR-basis current $I_{\mathrm{RR}}(\phi)$ violates the local conservation law and exhibits a nonsinusoidal curve due to inhomogeneous hopping strengths. Neither of these approaches can accurately describe the persistent current $I(\phi)$. However, the current $I(\phi)$ calculated using Eq. (1) aligns with exact diagonalization results that include a large reservoir. Compared to the current in the isolated ring, $I(\phi)$ is reduced because the positive current contributions from single-particle modes are diluted by dissipation-induced level broadening [90]. These conclusions remain consistent regardless of the number of reservoirs.

Finite temperature and interaction effects—First, we consider the effect of thermal fluctuations on the persistent current [91]. This requires integrating $\rho(\omega)$ over ω using $f_{\mathrm{FD}}(\omega, \beta) = 1/(e^{\beta\omega} + 1)$ with $\beta = 1/k_B T$ and k_B is the Boltzmann constant. Subsequently, $f_{\mathrm{eff}}(\varepsilon)$ in Eq. (5) is extended to form an effective NH Fermi-Dirac distribution at finite temperatures:

$$f_{\mathrm{eff}}(\varepsilon, \beta) = -\frac{1}{\pi}\left[\Psi\left(\frac{1}{2} + \frac{i\beta\varepsilon}{2\pi}\right) - \frac{i\pi}{2}\right], \tag{8}$$

where the digamma function Ψ [92] is defined as the derivative of the log-gamma function $\log\Gamma$ [93]. Using Eq. (8), we find that at finite temperatures, Eq. (1) becomes (see Supplemental Material [54]):

$$I(\phi, \beta) = \frac{2}{\beta}\frac{d}{d\phi}\mathrm{Re}\,\mathrm{Tr}\log\Gamma\left(\frac{1}{2} + \frac{i\beta}{2\pi}\mathcal{H}_{\mathrm{eff}}\right), \tag{9}$$

which extends the expression $\mathbf{2}\partial_\phi F$ for the persistent current, where F denotes the free energy in Hermitian systems [56], to encompass NH scenarios. As shown in Figs. 3(a) and 3(b), Eq. (9) includes Eq. (1) when at $T = 0$ and accurately matches the currents for $T \neq 0$ calculated by exact diagonalization. This indicates a decrease in currents for both systems as T increases. As illustrated in Fig. 3(c), such an excellent agreement is grounded on the fact that $\mathrm{Im} f_{\mathrm{eff}}(\varepsilon, \beta)$ in Eq. (8) will revert to $f_{\mathrm{FD}}(\varepsilon, \beta)$ as $\mathrm{Im}\varepsilon \to 0$. The smoothness of persistent currents near EPs can be attributed to the analytic properties of $f_{\mathrm{eff}}(\varepsilon, \beta)$ in the lower half of the complex plane [54].

To examine potential characteristics of EPs in the presence of many-body interactions, we introduce the electrostatic repulsion $H_{\mathrm{int}} = U \sum_{j\in\mathbb{N}} (n_j - 1/2)(n_{j+1} - 1/2)$, where U is the interaction strength. In such interacting scenarios, the first equality in Eq. (2) remains valid for the ground state. To maintain each reservoir as large as $N_E = 101$, we perform the density matrix renormalization group (DMRG) algorithm via DMRGpy [94]. Figures 3(d) and 3(e) show that as U increases, the amplitude of $I(\phi)$ in both systems will eventually be suppressed to zero due to the enhanced electron-electron scattering [95]. No signatures of EPs are detected in the current in any of the cases presented with respect to temperatures and interactions.

Current susceptibility—To elucidate the presence of EPs in systems with a phase-dependent spectrum, here we derive their linear response to a time-dependent phase driving $\phi(\tau) = \phi + \delta\phi(\tau)$, with $\delta\phi(\tau) \ll 1$. The current susceptibility that characterizes the response is given by [96–98]:

$$\Pi(\phi, \tau) = -\mathrm{i}\Theta(\tau)\langle[J(\tau), J(0)]\rangle. \tag{10}$$

We first transform Eq. (10) to the frequency space $\Pi(\phi, \omega) = \int \Pi(\phi, \tau)\mathrm{e}^{+\mathrm{i}\omega\tau}\mathrm{d}\tau$ and use the biorthogonal modes to obtain

$$\begin{aligned} \mathrm{Im}\Pi(\phi, \omega) &= \pi t_j^2 \mathrm{Re}[\mathbb{P}(\phi, +\omega) - \mathbb{P}(\phi, -\omega)], \\ \mathbb{P}(\phi, \omega) &= +P_{j+1,j,j+1,j}(\omega) - P_{j,j,j+1,j+1}(\omega) \\ &\quad + P_{j,j+1,j,j+1}(\omega) - P_{j+1,j+1,j,j}(\omega), \end{aligned} \tag{11}$$

with $P_{ijkl}(\omega) \equiv \int \langle i|\rho(\omega')|j\rangle\langle k|\rho(\omega+\omega')|l\rangle f_{\mathrm{FD}}(\omega')\mathrm{d}\omega'$. In the case of SNS junctions, $\mathbb{P}(\phi, \omega)$ contains four additional terms stemming from the contributions of the holes [99]. Nevertheless, the integral $P_{ijkl}(\omega)$ is shared by both systems and possesses an analytical expression at $T = 0$:

$$\begin{aligned} P_{ijkl}(\omega) &= \sum_{nm} \frac{p_{ijkl}^{nm-} + p_{ijkl}^{n\tilde{m}+} + p_{ijkl}^{\tilde{n}m-} + p_{ijkl}^{\tilde{n}\tilde{m}+}}{4}, \\ p_{ijkl}^{nm\pm} &\equiv -\frac{1}{\pi}\psi_{ni}^{\mathrm{R}}\psi_{nj}^{\mathrm{L}*}\psi_{mk}^{\mathrm{R}}\psi_{ml}^{\mathrm{L}*}\frac{f_{\mathrm{eff}}(\pm\epsilon_n) - f_{\mathrm{eff}}(\pm\epsilon_m \mp \omega)}{(\pm\epsilon_n) - (\pm\epsilon_m \mp \omega)}, \end{aligned} \tag{12}$$

where the tilde over m conjugates the m eigenvalue and exchange $\mathrm{L} \leftrightarrow \mathrm{R}$ on the m-biorthogonal wave functions. Equation (12) embeds $f_{\mathrm{eff}}(\epsilon)$ and reduces to the Hermitian case $P_{ijkl}(\omega) = \sum_{nm}\psi_{ni}\psi_{nj}^*\psi_{mk}\psi_{ml}^*\Theta(-\epsilon_n)\delta(\omega + \epsilon_n - \epsilon_m)$ in the decoupled limit $\kappa \to 0$. In NH systems, $\mathrm{Im}\Pi(\phi, \omega)$ will peak at level transitions $\omega = \mathrm{Re}\epsilon_m - \mathrm{Re}\epsilon_n$ with a larger linewidth due to a finite $\mathrm{Im}\epsilon_m$. As shown in Fig. 4, this broadened effect is more evident when transitions between levels encounter EPs. As κ/t increases, these peaks will be significantly enhanced and accumulate towards the regions between EPs. Our results agree with the full exact diagonalization [54] and are consistent with the Lindblad formalism [40]: (i) the effect of EPs cannot be observed in the steady state (including equilibrium); (ii) any manifestation of an EP has a dynamical nature.

Conclusions and outlook—In this Letter, we identified an effective distribution that captures the quantum many-body observables of NH fermionic systems in equilibrium. This distribution, derived microscopically from the biorthogonal Green's function, serves as an extension of the Fermi-Dirac distribution for NH systems. We utilized this formalism in the context of quantum transport and derived an analytical

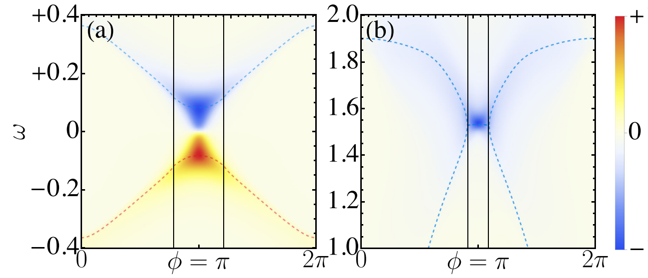

FIG. 4. Normalized imaginary part of current susceptibility $\Pi(\phi, \omega)$ of NH systems. (a) $\mathrm{Im}\Pi(\phi, \omega)$ for the SNS junction, incorporating negative ω to reflect the particle-hole symmetry. (b) $\mathrm{Im}\Pi(\phi, \omega)$ for the normal mesoscopic ring. Peaks of $\mathrm{Im}\Pi(\phi, \omega)$ correspond to energy level transitions (dashed lines) and are concentrated between two EPs (black lines). The parameters are the same as in Fig. 1.

equation for the persistent current flowing in SNS junctions and normal mesoscopic rings connected to reservoirs. We demonstrated that there are no anomalies in the persistent currents near EPs, showing that their amplitudes are suppressed by thermal fluctuations and many-body interactions. Our findings have been validated through exact diagonalization with excellent agreement. We conclude that the signatures of EPs are only discernible in a dynamical quantity—the current susceptibility—rather than a static observable.

Our formalism extends beyond quantum persistent current transport and holds promise for broader applications. It can be adapted to systems such as multi-Josephson junctions [100–102] and quantum spin chains [103], potentially unveiling new insights into their topological and entanglement characteristics. Furthermore, generalizing this formalism to encompass nonequilibrium scenarios, such as quantum pumps [104–106], shows great potential.

Note added—Our formalism fully agrees with the scattering matrix theory [107] and can be applied to calculating additional thermodynamic quantities [108].

Acknowledgments—We thank C. W. J. Beenakker, D.-L. Deng, W. Brzezicki, W.-T. Xue, L.-W. Yu, S.-Y. Zhang, W. Li, and Z. Liu for helpful discussions, and H.-R. Wang, in particular, for his valuable feedback from reading the first version of this manuscript. This work is supported by the Foundation for Polish Science project MagTop (No. FENG.02.01-IP.05-0028/23) co-financed by the European Union from the funds of Priority 2 of the European Funds for a Smart Economy Program 2021–2027 (FENG) and by the National Science Centre (Poland) OPUS Grant No. 2021/41/B/ST3/04475. P.-X. S. and Z. L. acknowledge support from the Tsinghua University Dushi Program and Shanghai Qi Zhi Institute. J. L. L. acknowledges the computational resources provided by the Aalto Science-IT project the financial support from the Academy of

Finland Projects No. 331342 and No. 358088. P.-X. S. acknowledges additional support from the European Union's Horizon Europe research and innovation programme under the Marie Skłodowska-Curie Grant Agreement No. 101180589 (SymPhysAI).

Views and opinions expressed are however those of the author(s) only and do not necessarily reflect those of the European Union or the European Research Executive Agency. Neither the European Union nor the granting authority can be held responsible for them.

Data availability—The codes used for this Letter are publicly available in GitHub [94].

[1] Y. Ashida, Z. Gong, and M. Ueda, Non-Hermitian physics, Adv. Phys. **69**, 249 (2020).
[2] E. J. Bergholtz, J. C. Budich, and F. K. Kunst, Exceptional topology of non-Hermitian systems, Rev. Mod. Phys. **93**, 015005 (2021).
[3] K. Ding, C. Fang, and G. Ma, Non-Hermitian topology and exceptional-point geometries, Nat. Rev. Phys. **4**, 745 (2022).
[4] N. Okuma and M. Sato, Non-Hermitian topological phenomena: A review, Annu. Rev. Condens. Matter Phys. **14**, 83 (2023).
[5] W.-T. Xue, M.-R. Li, Y.-M. Hu, F. Song, and Z. Wang, Simple formulas of directional amplification from non-Bloch band theory, Phys. Rev. B **103**, L241408 (2021).
[6] W.-T. Xue, Y.-M. Hu, F. Song, and Z. Wang, Non-Hermitian edge burst, Phys. Rev. Lett. **128**, 120401 (2022).
[7] Y.-M. Hu, W.-T. Xue, F. Song, and Z. Wang, Steady-state edge burst: From free-particle systems to interaction-induced phenomena, Phys. Rev. B **108**, 235422 (2023).
[8] B. Li, H.-R. Wang, F. Song, and Z. Wang, Non-Bloch dynamics and topology in a classical nonequilibrium process, Phys. Rev. B **109**, L201121 (2024).
[9] J. Zou, S. Bosco, E. Thingstad, J. Klinovaja, and D. Loss, Dissipative spin-wave diode and nonreciprocal magnonic amplifier, Phys. Rev. Lett. **132**, 036701 (2024).
[10] Y. Yu, L.-W. Yu, W. Zhang, H. Zhang, X. Ouyang, Y. Liu, D.-L. Deng, and L.-M. Duan, Experimental unsupervised learning of non-Hermitian knotted phases with solid-state spins, npj Quantum Inf. **8**, 116 (2022).
[11] G. Chen, F. Song, and J. L. Lado, Topological spin excitations in non-Hermitian spin chains with a generalized kernel polynomial algorithm, Phys. Rev. Lett. **130**, 100401 (2023).
[12] K. Ochkan, R. Chaturvedi, V. Könye, L. Veyrat, R. Giraud, D. Mailly, A. Cavanna, U. Gennser, E. M. Hankiewicz, B. Büchner, J. van den Brink, J. Dufouleur, and I. C. Fulga, Non-Hermitian topology in a multi-terminal quantum Hall device, Nat. Phys. **20**, 395 (2024).
[13] F. K. Kunst, E. Edvardsson, J. C. Budich, and E. J. Bergholtz, Biorthogonal bulk-boundary correspondence in non-Hermitian systems, Phys. Rev. Lett. **121**, 026808 (2018).
[14] S. Yao and Z. Wang, Edge states and topological invariants of non-Hermitian systems, Phys. Rev. Lett. **121**, 086803 (2018).
[15] S. Yao, F. Song, and Z. Wang, Non-Hermitian Chern bands, Phys. Rev. Lett. **121**, 136802 (2018).
[16] Z. Yang, K. Zhang, C. Fang, and J. Hu, Non-Hermitian bulk-boundary correspondence and auxiliary generalized brillouin zone theory, Phys. Rev. Lett. **125**, 226402 (2020).
[17] D. Bernard and A. LeClair, A Classification of Non-Hermitian random matrices, in *Statistical Field Theories*, NATO Science Series, edited by A. Cappelli and G. Mussardo (Springer Netherlands, Dordrecht, 2002), pp. 207–214.
[18] K. Kawabata, K. Shiozaki, M. Ueda, and M. Sato, Symmetry and topology in non-Hermitian physics, Phys. Rev. X **9**, 041015 (2019).
[19] A. Altland, M. Fleischhauer, and S. Diehl, Symmetry classes of open fermionic quantum matter, Phys. Rev. X **11**, 021037 (2021).
[20] L.-W. Yu and D.-L. Deng, Unsupervised learning of non-Hermitian topological phases, Phys. Rev. Lett. **126**, 240402 (2021).
[21] M. M. Denner, A. Skurativska, F. Schindler, M. H. Fischer, R. Thomale, T. Bzdušek, and T. Neupert, Exceptional topological insulators, Nat. Commun. **12**, 5681 (2021).
[22] T. Kato, *Perturbation Theory for Linear Operators*, 2nd ed., Classics in Mathematics (Springer-Verlag, Berlin Heidelberg, 1995).
[23] W. D. Heiss, The physics of exceptional points, J. Phys. A **45**, 444016 (2012).
[24] G. H. Golub and C. F. Van Loan, *Matrix Computations*, 4th ed. (The Johns Hopkins University Press, Baltimore, 2013).
[25] J. Wiersig, Enhancing the sensitivity of frequency and energy splitting detection by using exceptional points: Application to microcavity sensors for single-particle detection, Phys. Rev. Lett. **112**, 203901 (2014).
[26] W. Chen, Ş. Kaya Özdemir, G. Zhao, J. Wiersig, and L. Yang, Exceptional points enhance sensing in an optical microcavity, Nature (London) **548**, 192 (2017).
[27] H. Hodaei, A. U. Hassan, S. Wittek, H. Garcia-Gracia, R. El-Ganainy, D. N. Christodoulides, and M. Khajavikhan, Enhanced sensitivity at higher-order exceptional points, Nature (London) **548**, 187 (2017).
[28] H.-K. Lau and A. A. Clerk, Fundamental limits and non-reciprocal approaches in non-Hermitian quantum sensing, Nat. Commun. **9**, 4320 (2018).
[29] T. E. Lee, F. Reiter, and N. Moiseyev, Entanglement and spin squeezing in non-Hermitian phase transitions, Phys. Rev. Lett. **113**, 250401 (2014).
[30] P. San-Jose, J. Cayao, E. Prada, and R. Aguado, Majorana bound states from exceptional points in non-topological superconductors, Sci. Rep. **6**, 21427 (2016).
[31] Y. Ashida, S. Furukawa, and M. Ueda, Parity-time-symmetric quantum critical phenomena, Nat. Commun. **8**, 15791 (2017).
[32] Y. Tserkovnyak, Exceptional points in dissipatively coupled spin dynamics, Phys. Rev. Res. **2**, 013031 (2020).
[33] S. Kohler, J. Lehmann, and P. Hänggi, Driven quantum transport on the nanoscale, Phys. Rep. **406**, 379 (2005).
[34] S. Datta, *Quantum Transport: Atom to Transistor* (Cambridge University Press, Cambridge, England, 2005).

[35] G. T. Landi, D. Poletti, and G. Schaller, Nonequilibrium boundary-driven quantum systems: Models, methods, and properties, Rev. Mod. Phys. **94**, 045006 (2022).

[36] V. Gorini, A. Kossakowski, and E. C. G. Sudarshan, Completely positive dynamical semigroups of N-level systems, J. Math. Phys. (N.Y.) **17**, 821 (1976).

[37] G. Lindblad, On the generators of quantum dynamical semigroups, Commun. Math. Phys. **48**, 119 (1976).

[38] T. Prosen, Third quantization: A general method to solve master equations for quadratic open Fermi systems, New J. Phys. **10**, 043026 (2008).

[39] A. McDonald and A. A. Clerk, Third quantization of open quantum systems: Dissipative symmetries and connections to phase-space and Keldysh field-theory formulations, Phys. Rev. Res. **5**, 033107 (2023).

[40] F. Minganti, A. Miranowicz, R. W. Chhajlany, and F. Nori, Quantum exceptional points of non-Hermitian Hamiltonians and Liouvillians: The effects of quantum jumps, Phys. Rev. A **100**, 062131 (2019).

[41] A. McDonald, R. Hanai, and A. A. Clerk, Nonequilibrium stationary states of quantum non-Hermitian lattice models, Phys. Rev. B **105**, 064302 (2022).

[42] F. Song, S. Yao, and Z. Wang, Non-Hermitian skin effect and chiral damping in open quantum systems, Phys. Rev. Lett. **123**, 170401 (2019).

[43] G. Rickayzen, *Green's Functions and Condensed Matter* (Academic Press, New York, 1980).

[44] E. N. Economou, *Green's Functions in Quantum Physics*, 3rd ed. (Springer, New York, 2006).

[45] H. Wang, *Green's Function in Condensed Matter Physics*, 1st ed. (Alpha Science International, Oxford, UK, 2012).

[46] M. M. Odashima, B. G. Prado, and E. Vernek, Pedagogical introduction to equilibrium Green's functions: Condensed-matter examples with numerical implementations, Rev. Bras. Ensino Fís. **39**, 1 (2016).

[47] H. Shen and L. Fu, Quantum oscillation from in-gap states and a non-Hermitian Landau level problem, Phys. Rev. Lett. **121**, 026403 (2018).

[48] V. Kozii and L. Fu, Non-Hermitian topological theory of finite-lifetime quasiparticles: Prediction of bulk Fermi arc due to exceptional point, Phys. Rev. B **109**, 235139 (2024).

[49] V. Meden, L. Grunwald, and D. M. Kennes, $\mathcal{PT}$-symmetric, non-Hermitian quantum many-body physics—a methodological perspective, Rep. Prog. Phys. **86**, 124501 (2023).

[50] J. Cayao and M. Sato, Non-Hermitian phase-biased Josephson junctions, arXiv:2307.15472v1.

[51] C.-A. Li, H.-P. Sun, and B. Trauzettel, Anomalous Andreev spectrum and transport in non-Hermitian Josephson junctions, arXiv:2307.04789v3.

[52] V. Kornich, Current-voltage characteristics of the normal metal-insulator-PT-symmetric non-Hermitian superconductor junction as a probe of non-Hermitian formalisms, Phys. Rev. Lett. **131**, 116001 (2023).

[53] We adopt the LR/RR-basis definition in Ref. [52], where the electron density is anomalous at EPs, and the PT-symmetric Hamiltonian is distinct from $\mathcal{H}_{\mathrm{eff}}$ studied in this Letter within the context of open quantum systems [49].

[54] See Supplemental Material at http://link.aps.org/supplemental/10.1103/PhysRevLett.133.086301 for (i) Green's function and self-energy, (ii) properties of the NH Fermi-Dirac distribution, (iii) derivation of persistent current formula and its continuity at EPs, and (iv) extended numerical results on low-energy spectra, persistent currents, and current susceptibility, which includes Ref. [55].

[55] P.-X. Shen, V. Perrin, M. Trif, and P. Simon, Majorana-magnon interactions in topological Shiba chains, Phys. Rev. Res. **5**, 033207 (2023).

[56] C. W. J. Beenakker and H. van Houten, The superconducting quantum point contact, in *Nanostructures and Mesoscopic Systems*, edited by W. P. Kirk and M. A. Reed (Academic Press, New York, 1992), pp. 481–497.

[57] M. Büttiker, Small normal-metal loop coupled to an electron reservoir, Phys. Rev. B **32**, 1846 (1985).

[58] A. Stern, Y. Aharonov, and Y. Imry, Phase uncertainty and loss of interference: A general picture, Phys. Rev. A **41**, 3436 (1990).

[59] D. Loss and K. Mullen, Dephasing by a dynamic asymmetric environment, Phys. Rev. B **43**, 13252 (1991).

[60] L.-F. Chang and P. F. Bagwell, Control of Andreev-level occupation in a Josephson junction by a normal-metal probe, Phys. Rev. B **55**, 12678 (1997).

[61] N. A. Mortensen, A.-P. Jauho, and K. Flensberg, Dephasing in semiconductor–superconductor structures by coupling to a voltage probe, Superlattices Microstruct. **28**, 67 (2000).

[62] T. Gramespacher and M. Büttiker, Distribution functions and current-current correlations in normal-metal–superconductor heterostructures, Phys. Rev. B **61**, 8125 (2000).

[63] M. Belogolovskii, A. Golubov, M. Grajcar, M. Yu. Kupriyanov, and P. Seidel, Charge transport across a mesoscopic superconductor–normal metal junction: Coherence and decoherence effects, Physica (Amsterdam) **357–360C**, 1592 (2001).

[64] M. Belogolovskii, Phase-breaking effects in superconducting heterostructures, Phys. Rev. B **67**, 100503(R) (2003).

[65] B. Béri, Dephasing-enabled triplet Andreev conductance, Phys. Rev. B **79**, 245315 (2009).

[66] A.-P. Jauho, N. S. Wingreen, and Y. Meir, Time-dependent transport in interacting and noninteracting resonant-tunneling systems, Phys. Rev. B **50**, 5528 (1994).

[67] P. P. Potts, A. A. S. Kalaee, and A. Wacker, A thermodynamically consistent Markovian master equation beyond the secular approximation, New J. Phys. **23**, 123013 (2021).

[68] T. Yu, J. Zou, B. Zeng, J. W. Rao, and K. Xia, Non-Hermitian topological magnonics, Phys. Rep. **1062**, 1 (2024).

[69] D. C. Brody, Biorthogonal quantum mechanics, J. Phys. A **47**, 035305 (2013).

[70] Y. Chen and H. Zhai, Hall conductance of a non-Hermitian Chern insulator, Phys. Rev. B **98**, 245130 (2018).

[71] Z. Yang, Q. Yang, J. Hu, and D. E. Liu, Dissipative Floquet Majorana modes in proximity-induced topological superconductors, Phys. Rev. Lett. **126**, 086801 (2021).

[72] R. Arouca, J. Cayao, and A. M. Black-Schaffer, Topological superconductivity enhanced by exceptional points, Phys. Rev. B **108**, L060506 (2023).

[73] The $\ln|\varepsilon_n|$ term stems from the principal value (PV) in the integrand, which is typically disregarded in the literature [43], since $|\psi_n^{\mathrm{L}}\rangle \approx |\psi_n^{\mathrm{R}}\rangle$ in the weak coupling limit.

However, PV plays a crucial role in correctly determining observables in EPs, which typically occur in the strong coupling regime.

[74] Observables are gauge-invariant under $f_{\text{eff}} \to f_{\text{eff}} + \mathbb{R}$: All observables stay the same with $f_{\text{eff}}(\varepsilon) = -(1/\pi)\ln(\varepsilon/C)$, $\forall\ C \in \mathbb{R}$ [54]. Hence, we set $C = 1$ for simplicity.

[75] Owing to the analytic property of f_{eff}, the EP is a removable singularity for physical observables, albeit a branch point for biorthogonal wave functions [54].

[76] K. Kawabata, T. Numasawa, and S. Ryu, Entanglement phase transition induced by the non-Hermitian skin effect, Phys. Rev. X **13**, 021007 (2023).

[77] L. Herviou, N. Regnault, and J. H. Bardarson, Entanglement spectrum and symmetries in non-Hermitian fermionic non-interacting models, SciPost Phys. **7**, 069 (2019).

[78] M. Naghiloo, M. Abbasi, Y. N. Joglekar, and K. W. Murch, Quantum state tomography across the exceptional point in a single dissipative qubit, Nat. Phys. **15**, 1232 (2019).

[79] M. Büttiker, Y. Imry, and R. Landauer, Josephson behavior in small normal one-dimensional rings, Phys. Lett. **96A**, 365 (1983).

[80] L. P. Lévy, G. Dolan, J. Dunsmuir, and H. Bouchiat, Magnetization of mesoscopic copper rings: Evidence for persistent currents, Phys. Rev. Lett. **64**, 2074 (1990).

[81] H. Bary-Soroker, O. Entin-Wohlman, and Y. Imry, Effect of pair breaking on mesoscopic persistent currents well above the superconducting transition temperature, Phys. Rev. Lett. **101**, 057001 (2008).

[82] H. Bluhm, N. C. Koshnick, J. A. Bert, M. E. Huber, and K. A. Moler, Persistent currents in normal metal rings, Phys. Rev. Lett. **102**, 136802 (2009).

[83] A. C. Bleszynski-Jayich, W. E. Shanks, B. Peaudecerf, E. Ginossar, F. von Oppen, L. Glazman, and J. G. E. Harris, Persistent currents in normal metal rings, Science **326**, 272 (2009).

[84] J. P. Carini, K. A. Muttalib, and S. R. Nagel, Origin of the Bohm-Aharonov effect with half flux quanta, Phys. Rev. Lett. **53**, 102 (1984).

[85] D. A. Browne, J. P. Carini, K. A. Muttalib, and S. R. Nagel, Periodicity of transport coefficients with half flux quanta in the Aharonov-Bohm effect, Phys. Rev. B **30**, 6798 (1984).

[86] H.-F. Cheung, Y. Gefen, E. K. Riedel, and W.-H. Shih, Persistent currents in small one-dimensional metal rings, Phys. Rev. B **37**, 6050 (1988).

[87] N. Byers and C. N. Yang, Theoretical considerations concerning quantized magnetic flux in superconducting cylinders, Phys. Rev. Lett. **7**, 46 (1961).

[88] $\{t_j\}_{j=1}^{6} = \{-0.859915, -0.884918, -0.918446, -0.846311, -1.19937, -0.984676\}$ for numerical results in the Letter.

[89] E. Akkermans, A. Auerbach, J. E. Avron, and B. Shapiro, Relation between persistent currents and the scattering matrix, Phys. Rev. Lett. **66**, 76 (1991).

[90] R. Landauer and M. Büttiker, Resistance of small metallic loops, Phys. Rev. Lett. **54**, 2049 (1985).

[91] To maintain a unified formalism across normal rings and SNS junctions, we adopt a constant Δ and refrain from self-consistent calculations of observables for SNS junctions.

[92] E. W. Weisstein, Digamma Function (2024), https://functions.wolfram.com/GammaBetaErf/PolyGamma/introductions/DifferentiatedGammas/ShowAll.html.

[93] E. W. Weisstein, LogGamma Function (2024), https://functions.wolfram.com/GammaBetaErf/LogGamma/introductions/Gammas/ShowAll.html.

[94] The source code is available at https://github.com/peixinshen/NonHermitianFermiDiracDistributionPersistentCurrent.

[95] In the moderate range U, the current amplitude may fluctuate in normal rings due to the shift of the effective Fermi level.

[96] N. Trivedi and D. A. Browne, Mesoscopic ring in a magnetic field: Reactive and dissipative response, Phys. Rev. B **38**, 9581 (1988).

[97] M. Ferrier, B. Dassonneville, S. Guéron, and H. Bouchiat, Phase-dependent Andreev spectrum in a diffusive SNS junction: Static and dynamic current response, Phys. Rev. B **88**, 174505 (2013).

[98] B. Dassonneville, M. Ferrier, S. Guéron, and H. Bouchiat, Dissipation and supercurrent fluctuations in a diffusive normal-metal–superconductor ring, Phys. Rev. Lett. **110**, 217001 (2013).

[99] The four additional anomalous contributions are

$$+P_{N+j+1,j,j+1,N+j}(\omega) - P_{N+j,j,j+1,N+j+1}(\omega)$$
$$+P_{N+j,j+1,j,N+j+1}(\omega) - P_{N+j+1,j+1,j,N+j}(\omega).$$

Because of the local conservation law, $\mathbb{P}(\phi,\omega)$ is uniform $\forall\ j \in \mathbb{N}$ and thus we set j as the first site of $\mathbb{N}$ in the calculation.

[100] R.-P. Riwar, M. Houzet, J. S. Meyer, and Y. V. Nazarov, Multi-terminal Josephson junctions as topological matter, Nat. Commun. **7**, 11167 (2016).

[101] N. Pankratova, H. Lee, R. Kuzmin, K. Wickramasinghe, W. Mayer, J. Yuan, M. G. Vavilov, J. Shabani, and V. E. Manucharyan, Multiterminal Josephson effect, Phys. Rev. X **10**, 031051 (2020).

[102] M. Coraiola, D. Z. Haxell, D. Sabonis, H. Weisbrich, A. E. Svetogorov, M. Hinderling, S. C. ten Kate, E. Cheah, F. Krizek, R. Schott, W. Wegscheider, J. C. Cuevas, W. Belzig, and F. Nichele, Phase-engineering the Andreev band structure of a three-terminal Josephson junction, Nat. Commun. **14**, 6784 (2023).

[103] P.-X. Shen, S. Hoffman, and M. Trif, Theory of topological spin Josephson junctions, Phys. Rev. Res. **3**, 013003 (2021).

[104] M. Moskalets and M. Büttiker, Floquet scattering theory of quantum pumps, Phys. Rev. B **66**, 205320 (2002).

[105] M. Blaauboer, Charge pumping in mesoscopic systems coupled to a superconducting lead, Phys. Rev. B **65**, 235318 (2002).

[106] V. F. Becerra, M. Trif, and T. Hyart, Quantized spin pumping in topological ferromagnetic-superconducting nanowires, Phys. Rev. Lett. **130**, 237002 (2023).

[107] C. W. J. Beenakker, Josephson effect in a junction coupled to an electron reservoir, arXiv:2404.13976.

[108] D. M. Pino, Y. Meir, and R. Aguado, Thermodynamics of non-Hermitian Josephson junctions with exceptional points, arXiv:2405.02387.